

# Synthesis, Characterization and Antibacterial Activity of Mixed Ligand (HL) Complexes Mn(II), Co(II), Ni(II), Zn(II), Cd(II) and Hg(II) with Azide ( $\text{N}_3^-$ )

Jassim S. Sultan, Sajed M. Lateaf, Dhuha K. Rashid

Department of Chemistry, College of Education for pure Sciences, Ibn Al-Hiatham, University of Baghdad, Baghdad, Iraq  
Email: [ja.sultan@yahoo.com](mailto:ja.sultan@yahoo.com)

Received 12 June 2015; accepted 5 October 2015; published 8 October 2015

Copyright © 2015 by authors and Scientific Research Publishing Inc.  
This work is licensed under the Creative Commons Attribution International License (CC BY).  
<http://creativecommons.org/licenses/by/4.0/>



Open Access

---

## Abstract

The complexes of mixed ligand (HL) as primary ligand with azide ion ( $\text{N}_3^-$ ) as co-ligand with Mn(II), Co(II), Ni(II), Zn(II), Cd(II) and Hg(II) were prepared via reaction metal (II) chloride salt with ligand (HL) and sodium azide ( $\text{NaN}_3$ ) using 1:2:2 mole ratio in ethanol solvent, respectively. The complexes of mixed ligand (HL) were characterized by elemental microanalysis (C.H.N), atomic absorption chloride content, molar conductance, magnetic susceptibility, melting point, FTIR and UV-Vis spectral data. The anti bacterial activity with four kinds of bacteria, *Staphylococcus aureus*, *Bacillus*, *Escherichia coli* and *Pseudomonas aureus* was studied.

## Keywords

4-Aminoantipyrine, Glyoxylic Acid, Sodium Azide, Schiff Base, Azido Mixed Ligand

---

## 1. Introduction

The chemistry of Schiff bases metal complexes is of interest because these species display a variety of reactivity mode and they possess catalytic and biological activity [1]. Metal complexes of nitrogen-oxygen chelating agents derived from 4-aminoantipyrine Schiff bases have been studied extensively due to their pronounced applications in biological, clinical, analytical and pharmacological areas [2]-[4].

4-Aminoantipyrine, an antipyretic agent [5] is one of the pyrazole derivatives. Numerous synthetic compounds containing pyrazole moiety have been focused in the field of medicinal chemistry [6] because of their

**How to cite this paper:** Sultan, J.S., Lateaf, S.M. and Rashid, D.K. (2015) Synthesis, Characterization and Antibacterial Activity of Mixed Ligand (HL) Complexes Mn(II), Co(II), Ni(II), Zn(II), Cd(II) and Hg(II) with Azide ( $\text{N}_3^-$ ). *Open Journal of Inorganic Chemistry*, 5, 102-111. <http://dx.doi.org/10.4236/ojic.2015.54011>

pharmacological, photographic, catalytic and liquid crystals applications [7] [8]. Glyoxylic acid and its derivatives play important roles in natural processes participating in the glyoxylate cycle which functions in plants and some microorganisms [9]. It has been widely used in organic synthesis for the manufacture of intermediate products in pharmaceutical [10]. The spectrophotometric methods are usually based on the reactivity of the aldehyde group [11] [12]. Azido-mixed ligand complexes particular interest has been focused on the azido ligand ( $\text{N}_3^-$ ) not only for its efficiency in ferromagnetic or antiferromagnetic coupling but also for its diversity in coordination modes,  $\mu-1, 1$ , (end-on EO),  $\mu-1, 3$  (end-end, EE),  $\mu-1, 1, 1, \mu-1, 1, 3$  or still other modes and polymeric bridging network, and a large number of azido-bridged complexes with different dimensionalities and various topologies have been reported in the literature [13] [14]. Polynuclear complexes and coordination polymer in which paramagnetic metal ions are bridged by short ligands have attracted great attention in recent years. The studies focusing on better understanding fundamental magnetic applications, a large number of azido-bridged transition metal complexes, have been reported [15].

## 2. Experimental

All chemicals were purchased from BDH, and used without further purifications.

### 2.1. Instrumentation

FTIR spectra were recorded in KBr on Shimadzu-8300 Spectrophotometer in the range of (4000 - 400  $\text{cm}^{-1}$ ). The electronic spectra in  $\text{H}_2\text{O}$  were recorded using the UV-Visible spectrophotometer type (spectra 190 - 900 nm) CECIL, England, with quartz cell of (1 cm) path length. The melting point was recorded on Gallen kamp Melting point Apparatus.

The Conductance Measurements were recorded on W. T. W. conductivity Meter. The metal contents of the complexes were determined by atomic absorption (A. A.) technique using a Shimadzu PR-5 with Orphic Printer atomic absorption spectrophotometer. Balance Magnetic Susceptibility model MSB-MLI was conducted for measuring the magnetic susceptibility.

The characterization of the new ligand (L) is achieved by  $^1\text{H}$  and  $^{13}\text{C}$ -NMR spectra were recorded by using a Bruker 300 MHz (Switzerland). Chemical Shift of all  $^1\text{H}$  and  $^{13}\text{C}$ -NMR spectra were recorded in  $\delta$ (ppm) unit downfield from internal reference tetramethylsilane (TMS), using  $\text{D}_2\text{O}$  as a solvent. Elemental analysis for carbon, hydrogen was performed using a Euro Vector EA 3000 A Elemental Analysis (Italy).

### 2.2. Synthesis of Ligand and Complexes

#### 2.2.1. Synthesis of Ligand (1,5-Dimethyl-3-oxo-2-phenyl-2,3-dihydro-1H-pyrazol-4-ylimino) (HL)

A solution of (4-AAP) (0.203 g, 1 mmole) in ethanol (20 ml), and a few drop of 48% of HBr, was added to a solution of (Glyoxylic acid) (0.074 g, 1 mmol) in ethanol (10 ml). The mixture was refluxed for (6 hr) with stirring. The resulting was an orange solution allowed to cool and dried at room temperature, then washed with ethanol and re-crystallization to the precipitate with methanol/ $\text{H}_2\text{O}$  to give orange crystals during (24 hr), m.p. (128 - 132) $^\circ\text{C}$ .

#### 2.2.2. Synthesis of $[\text{Co}(\text{HL})_2(\text{N}_3)_2] \cdot 2\text{H}_2\text{O}$ Complex

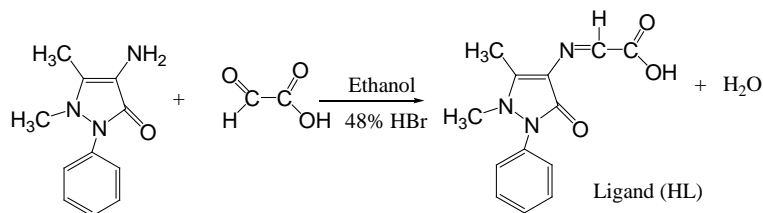
A solution of (HL) (0.518 g, 2 mmole) in ethanol (5 ml) and a solution of  $\text{NaN}_3$  (0.13 g, 2 mmol) in ethanol (5 ml) were added to a stirred solution of  $\text{CoCl}_2 \cdot 6\text{H}_2\text{O}$  (0.238 g, 1 mmol) in ethanol (5 ml). The resulting mixture was stirred for (1 hr). Then the mixture was filtered and dried then the precipitate was washed with an excess of ethanol and dried at room temperature during (24 hr). A pale green crystals were obtained, m.p. (116 - 121) $^\circ\text{C}$ . A similar method was used to prepare of Mn(II), Ni(II), Zn(II), Cd(II) and Hg(II) mixed ligand complexes.

## 3. Results and Discussion

### 3.1. Characterization of Ligand (HL)

In this study, new Schiff base ligand (HL) type (NOO) donor atoms was synthesized according to the used method shown in **Scheme 1**.

Spectroscopic methods [FT-IR, UV-Vis,  $^1\text{H}$  NMR,  $^{13}\text{C}$  NMR] along with melting point and elemental micro-analysis C.H.N. were used to characterization the new ligand (HL).



**Scheme 1.** Synthesis route of ligand (HL).

### 3.1.1. $^1\text{H}$ NMR Spectral Data

The  $^1\text{H}$ -NMR spectrum of ligand (HL) shows single peaks attributed to two methyl groups appeared at range ( $\delta$ 1.06 -  $\delta$ 2.91) ppm. The strong signal obtained at ( $\delta$ 3.35) ppm. due to DMSO- $d_6$ . The weak peak at ( $\delta$ 8.14) ppm was attributed to proton of azomethine group (-N=CH-). Single weak peak attributed to proton of (-COOH) appeared at ( $\delta$ 9.30) ppm. The multiple chemical shifts around (6.98 - 7.47) ppm may assigned to aromatic protons. The two weak signals at  $\delta$ (3.04) and  $\delta$ (3.14) ppm refer to water molecule of DMSO [16].

### 3.1.2. $^{13}\text{C}$ NMR Spectral Data

$^{13}\text{C}$  NMR spectrum of ligand (HL) shows chemical shifts at (15.54) ppm and (18.35) ppm refer to  $\text{C}_5$  and  $\text{C}_6$  for two  $\text{CH}_3$  group respectively. The chemical shifts at (61.79) ppm and (88.32) ppm were attributed to  $\text{C}_3$  and  $\text{C}_4$  of C=C in 4-AAP ring respectively. Signals related to aromatic carbon ( $\text{C}_7$  -  $\text{C}_{12}$ ) were detected at range (126.04 - 130.89) ppm. The chemical shift of  $\text{C}_1$  for carboxylic group appeared as expected downfield at (170.25) ppm. The two chemical shift at (165.51) ppm and (135.47) ppm were attributed to  $\text{C}_2$  for azomethine group (-N=CH-) and  $\text{C}_{13}$  to C=O for 4-AAP respectively. Finally, the chemical shift at (40.86) ppm is due to DMSO  $d_6$  [17].

## 3.2. Characterization of Mixed Ligand (HL) Complexes with Azide ( $\text{N}_3^-$ )

The complexes of mixed ligand, (HL) as primary ligand with azide ion ( $\text{N}_3^-$ ) as co-ligand with Mn(II), Co(II), Ni(II), Zn(II), Cd(II) and Hg(II) were prepared via reaction metal (II) chloride salt with ligand (HL) and sodium azide ( $\text{NaN}_3$ ) using 1:2:2 mole ratio in ethanol solvent respectively. The method of this synthesis shows in **Scheme 2** and **Scheme 3**.

Spectroscopic methods [FT-IR, UV-Vis, A. A.] along with molar conductivity, elemental microanalysis C.H.N, Chloride content, magnetic susceptibility, melting point were used to characterize the prepared mixed ligand complexes. All mixed ligand complexes are stable in solution and soluble in methanol, ethanol, acetone, DMSO and DMF solvents. Some physical properties were listed in **Table 1**. Elemental microanalysis C.H.N, metal and chloride analysis are in a good agreement with calculated values, **Table 2**.

### 3.2.1. Molar Conductance

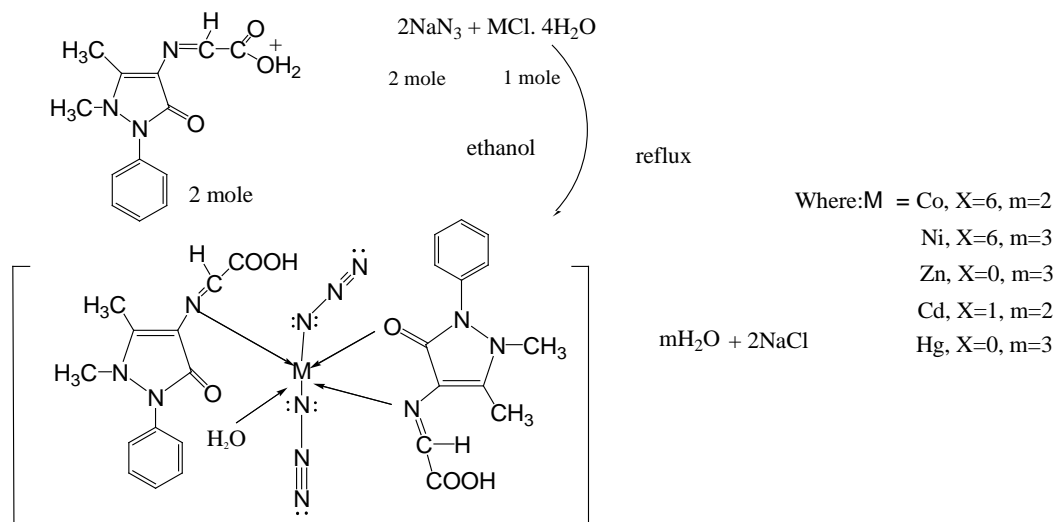
The molar conductance values, **Table 1**, of the soluble mixed ligand complexes in DMSO solvent in  $10^{-3}$  M solution at room temperature refer to non-electrolytic nature [18].

### 3.2.2. Magnetic Susceptibility

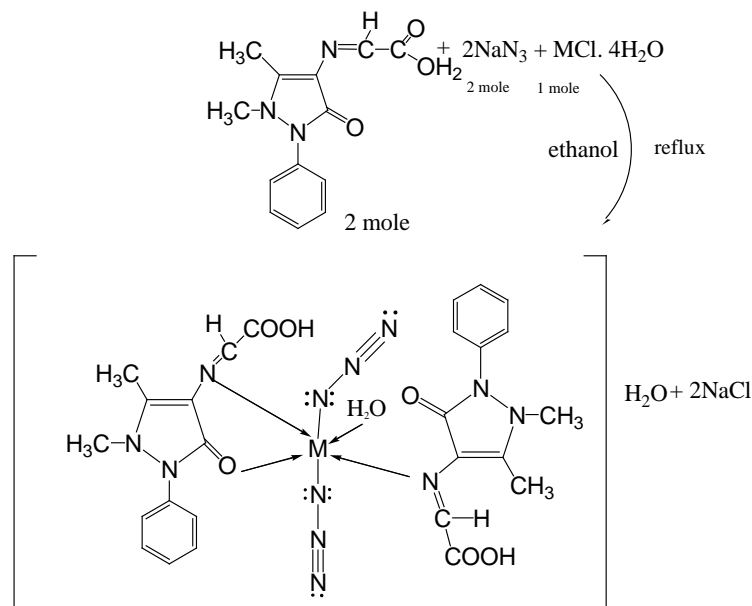
The magnetic susceptibility for all complexes were measured at room temperature and the effective magnetic moment ( $\mu_{\text{eff}}$ ) values [19] were listed in **Table 3**.

### 3.2.3. FT-IR Spectral Data

The IR spectra of mixed ligand complexes Co(II), Ni(II), Zn(II), Cd(II), and Hg(II), exhibited band at (1616)  $\text{cm}^{-1}$ , (1624)  $\text{cm}^{-1}$ , (1614)  $\text{cm}^{-1}$ , (1616)  $\text{cm}^{-1}$ , and (1635)  $\text{cm}^{-1}$ , respectively, refers to stretching frequency  $\nu_{\text{C=O}}$  of 4-AAP ring, which was shifted to lower frequency when its comparison with that of the free ligand (HL), showing that the coordination between oxygen atom of this group with metal ion has happened [20]. The IR spectrum of mixed ligand complex of Mn(II), showed no change in position of the stretching frequency of  $\nu_{\text{C=O}}$  ring when it compare of free ligand, indicating that the oxygen atom of (C=O) ring wasn't involved in coordination with Mn(II). The detected bands at (1593)  $\text{cm}^{-1}$ , (1591)  $\text{cm}^{-1}$ , (1593)  $\text{cm}^{-1}$ , (1591)  $\text{cm}^{-1}$ , (1591)  $\text{cm}^{-1}$ , and (1591)  $\text{cm}^{-1}$  in the IR spectra of all mixed ligand complexes refer to stretching frequency of imine



**Scheme 2.** Synthesis route of mixed ligand complexes for Co(II), Ni(II), Zn(II), Cd(II) and Hg(II).



**Scheme 3.** Synthesis route of mixed ligand (HL) complex for  $[\text{Mn}(\text{HL})_2(\text{N}_3)_2(\text{H}_2\text{O})_2] \cdot \text{H}_2\text{O}$ .

**Table 1.** Some physical properties and molar conductance (M.C) of mixed ligand (HL) complexes.

Complexes	M.wt g/mol	Yield %	Colour	M. P. °C	M.C $\text{ohm}^{-1} \cdot \text{cm}^2 \cdot \text{mol}^{-1}$
$[\text{Mn}(\text{HL})_2(\text{N}_3)_2(\text{H}_2\text{O})] \cdot \text{H}_2\text{O}$	711	78	Dark green	100	12.22
$[\text{Co}(\text{HL})_2(\text{N}_3)_2] \cdot 2\text{H}_2\text{O}$	697	91	Pale green	120	9.42
$[\text{Ni}(\text{HL})_2(\text{N}_3)_2] \cdot 3\text{H}_2\text{O}$	714.7	92	Pale olive	122	15.58
$[\text{Zn}(\text{HL})_2(\text{N}_3)_2] \cdot 3\text{H}_2\text{O}$	721.4	88	Pale orange	dec. 108 - 112	7.97
$[\text{Cd}(\text{HL})_2(\text{N}_3)_2] \cdot 2\text{H}_2\text{O}$	750.4	89	Pale orange	103	9.21
$[\text{Hg}(\text{HL})_2(\text{N}_3)_2] \cdot 3\text{H}_2\text{O}$	856.6	92	Pale orange	102	9.16

**Table 2.** Elemental microanalysis of mixed ligand (HL) complexes.

Complexes	Found, (cal cu.)%				
	C	H	N	M	Cl
[Mn(HL) <sub>2</sub> (N <sub>3</sub> ) <sub>2</sub> (H <sub>2</sub> O)]·H <sub>2</sub> O	(43.88) 43.06	(4.50) 3.85	(23.62) 23.84	(7.73) 7.26	Nil
[Co(HL) <sub>2</sub> (N <sub>3</sub> ) <sub>2</sub> (H <sub>2</sub> O) <sub>2</sub> ]·H <sub>2</sub> O	(44.76) 44.03	(4.01) 4.26	(24.10) 23.67	(8.46) 8.01	Nil
[Ni(HL) <sub>2</sub> (N <sub>3</sub> ) <sub>2</sub> ]·3H <sub>2</sub> O	(43.65) 42.86	(4.47) 3.82	(23.50) 22.64	(8.21) 7.75	Nil
[Zn(HL) <sub>2</sub> (N <sub>3</sub> ) <sub>2</sub> ]·3H <sub>2</sub> O	(43.24) 42.75	(4.43) 4.68	(23.28) 22.85	(9.06) 8.42	Nil
[Cd(HL) <sub>2</sub> (N <sub>3</sub> ) <sub>2</sub> ]·2H <sub>2</sub> O	(41.57) 40.82	(3.99) 3.52	(22.38) 23.04	(14.97) 14.62	Nil
[Hg(HL) <sub>2</sub> (N <sub>3</sub> ) <sub>2</sub> ]·3H <sub>2</sub> O	(36.42) 35.86	(3.73) 3.25	(19.61) 19.18	(23.41) 22.94	Nil

**Table 3.** Magnetic susceptibility and  $\mu_{\text{eff}}$  (B.M) of some mixed ligand (HL) complexes.

Complexes*	$X_g \times 10^{-6}$	$X_M \times 10^{-6}$	$X_A \times 10^{-6}$	$\mu_{\text{eff}}$ (B.M)	Suggested structure
[Mn(HL) <sub>2</sub> (N <sub>3</sub> ) <sub>2</sub> (H <sub>2</sub> O) <sub>2</sub> ]·H <sub>2</sub> O	18.57	13204.65	12971.03	5.56	Octahedral
[Co(HL) <sub>2</sub> (N <sub>3</sub> ) <sub>2</sub> ]·2H <sub>2</sub> O	14.08	9815.38	10049.0	4.88	Octahedral
[Ni(HL) <sub>2</sub> (N <sub>3</sub> ) <sub>2</sub> ]·3H <sub>2</sub> O	4.50	3217.88	3451.50	2.86	Octahedral

group (-N=CH-) which were shifted to lower frequency when it compare with that of free ligand showing that the coordination with the metal ions was occurred via nitrogen atom of imine group (-N=CH-) [21]. The IR spectra of all mixed ligand complexes exhibited new strong splitted band or new strong singlate band which wasn't observed in the IR spectrum of free ligand (HL), this band was located at (2123 cm<sup>-1</sup>, 2058 cm<sup>-1</sup>) Mn(II), (2123 cm<sup>-1</sup>, 2102 cm<sup>-1</sup>) Co(II), (2121 cm<sup>-1</sup>, 2036 cm<sup>-1</sup>) Ni(II), (2125 cm<sup>-1</sup>, 2036 cm<sup>-1</sup>) Hg(II), (2065) cm<sup>-1</sup> for Zn(II) and Cd(II), which was attributed to stretching frequency  $\nu_{\text{asy.}}(\text{N}_3^-)$ . While the new band at (1311) cm<sup>-1</sup> for Mn(II) Co(II) and at (1317) cm<sup>-1</sup> for Zn(II), Cd(II) and at (1313) cm<sup>-1</sup> for Hg(II), was attributed to stretching frequency  $\nu_{\text{sy.}}(\text{N}_3^-)$  [22]. These values of  $\nu_{\text{asy.}}(\text{N}_3^-)$  and  $\nu_{\text{sy.}}(\text{N}_3^-)$  suggest the coordination between azide ion ( $\text{N}_3^-$ ) and metal ion. Further, the two bands observed at (1419) cm<sup>-1</sup> and (1369) cm<sup>-1</sup> in the IR spectrum of free ligand which are assigned to  $\nu_{\text{asy.}}(\text{COO}^-)$  and  $\nu_{\text{sy.}}(\text{COO}^-)$  respectively, parically no or slightly change on these frequencies at complexation was observed, indicating noninvolvement of this group in coordination with metal ion [23]. In the IR spectra of mixed ligand complexes of Mn(II), Co(II), Ni(II), Zn(II), Cd(II), and Hg(II) abroad band was observed around (3464) cm<sup>-1</sup> to (3390) cm<sup>-1</sup> which was assigned to hydrate water molecules [24], while the presence of coordinated water (aqua) in the structure of Mn(II) complex was suggested by a broad band at (3390) cm<sup>-1</sup> and weak band at (931) cm<sup>-1</sup> in the IR spectrum of Mn(II) complex, which refer to  $\nu\text{O-H}$  and  $\delta\text{O-H}$  for H<sub>2</sub>O coordination molecules [25]. The stretching frequency of  $\nu\text{C=O}$  for carboxylate group in IR spectra for all mixed complexes appeared as overlap with band of  $\nu\text{C=O}$  ring or as a weak band around (1735) cm<sup>-1</sup>. Two bands in the region (545 - 505) cm<sup>-1</sup> and (505 - 445) cm<sup>-1</sup> typical for the presence of M-N and M-O in the IR spectra for all mixed ligand complexes as new bands [26]. These Two bands were not present in the spectrum of free ligand (HL). Other bands in the IR for all complexes were listed in **Table 4**. These observation in the IR spectra of free ligand and its mixed complexes indicate that the ligand (HL) coordinate with Co(II), Ni(II), Zn(II), Cd(II), and Hg(II) via oxygen atom of (C=O) ring and nitrogen atom of imine group (-N=CH-), behaving bidentate ligand. But its behaves as monodentate ligand when it coordinate with Mn(II) via nitrogen atom of imine group (-N=CH-) only. While the azide ion ( $\text{N}_3^-$ ) coordinates with metal ion in all mixed ligand complexes as terminal ligand. According to these fact, the primary oxidation states of the metal ions Mn(II), Co(II), Ni(II), Zn(II), Cd(II), and Hg(II) were satisfied by the presence of azide ion ( $\text{N}_3^-$ ) present inside the coordination sphere, that was proved by molar conductance values which were a good evidence for non-electrolytic complexes.

### 3.2.4. UV-Vis Spectral Data

The electronic spectral data for all mixed ligand complexes are summarized in **Table 5**, together with electronic

**Table 4.** The FT-IR spectral data (cm<sup>-1</sup>) of ligand (HL) and its mixed complexes.

Compounds	$\nu_{\text{O-H}}$	$\nu_{\text{C=O}}$ ring	$\nu_{\text{C=O}}$ carbox.	$\nu_{\text{N=C}}$ imine	$\nu_{\text{COO}^-}$ asy.	$\nu_{\text{COO}^-}$ sy.	$\nu_{\text{N}_3^-}$ asy.	$\nu_{\text{N}_3^-}$ sy.	$\nu_{\text{C=C}}$ arom.	$\nu_{\text{C-H}}$ arom.	$\nu_{\text{C-C}}$ aliph.	$\nu_{\text{C-H}}$ aliph.	$\nu_{\text{M-N}}$	$\nu_{\text{M-O}}$
(HL)	3421	1645	1724	1608	1419	1369	-	-	1586	2939	1197	2900	-	-
[Mn(HL) <sub>2</sub> (N <sub>3</sub> ) <sub>2</sub> (H <sub>2</sub> O) <sub>2</sub> ].H <sub>2</sub> O	3390	1647	Overlap	1593	1417	1369	2123 2058	1311	1570	3064	1190	2927	543	505
[Co(HL) <sub>2</sub> (N <sub>3</sub> ) <sub>2</sub> ].H <sub>2</sub> O	3442	1616	Overlap	1591	1421	1371	2123 2102	1311	1573	Overlap	1197	2935	505	445
[Ni(HL) <sub>2</sub> (N <sub>3</sub> ) <sub>2</sub> ].3H <sub>2</sub> O	3390	1624	1735	1593	1417	1363	2121 2036	1311	1575	Overlap	1168	Overlap	545	475
[Zn(HL) <sub>2</sub> (N <sub>3</sub> ) <sub>2</sub> ].3H <sub>2</sub> O	3464	1614	1735	1591	1417	1373	2065	1317	1560	3066	1141	2933	542	445
[Cd(HL) <sub>2</sub> (N <sub>3</sub> ) <sub>2</sub> ].2H <sub>2</sub> O	3446	1616	Overlap	1591	1419	1375	2065	1317	1558	3064	1188	2930	505	460
[Hg(HL) <sub>2</sub> (N <sub>3</sub> ) <sub>2</sub> ].3H <sub>2</sub> O	3346	1635	Overlap	1591	1417	1369	2125 2036	1313	1558	3064	1188	2900	505	453

**Table 5.** Electronic spectral data of ligand (HL) and its mixed complexes.

Compound	$\lambda_{\text{nm}}$	$\nu^-$ (cm <sup>-1</sup> )	( $\epsilon_{\text{max}}$ , molar <sup>-1</sup> .L.cm <sup>-1</sup> )	Electronic transition	Suggested structure
(HL)	276	36,231	1885	$\pi \rightarrow \pi^*$	-
	346	28,901	614	$n \rightarrow \pi^*$	
	362	27,624	500	$n \rightarrow \pi^*$	
	297	33,670	2370	Intra-ligand	
	345	28,986	2042	Intra-ligand	
[Mn(HL) <sub>2</sub> (N <sub>3</sub> ) <sub>2</sub> (H <sub>2</sub> O) <sub>2</sub> ].H <sub>2</sub> O	359	27,855	1324	Intra-ligand	Oh
	475	21,053	208	${}^6A_{1g} \rightarrow {}^4T_{2g}(G)$	
	638	15,674	41	${}^6A_{1g} \rightarrow {}^4T_{1g}(G)$	
	794	12,594	7	${}^6A_{1g} \rightarrow {}^4E_g(D)$	
	286	34,965	2304	Intra-ligand	
	345	28,986	2034	Intra-ligand	
[Co(HL) <sub>2</sub> (N <sub>3</sub> ) <sub>2</sub> ].2H <sub>2</sub> O	362	27,624	1228	Intra-ligand	oh
	650	15,387	13	${}^4T_{1g} \rightarrow {}^4A_{2g}$	
	879	11,377	4	${}^4T_{1g} \rightarrow {}^4T_{2g}$	
	281	35,587	2218	Intra-ligand	
[Ni(HL) <sub>2</sub> (N <sub>3</sub> ) <sub>2</sub> ].3H <sub>2</sub> O	347	28,818	1152	Intra-ligand	Oh
	365	27,397	842	Intra-ligand	
	426	23,474	323	${}^3A_{1g} \rightarrow {}^3T_{2g}(P)$	
	792	15,942	10	${}^3A_{1g} \rightarrow {}^3T_{1g}$	
[Zn(HL) <sub>2</sub> (N <sub>3</sub> ) <sub>2</sub> ].3H <sub>2</sub> O	879	11,377	2	${}^3A_{1g} \rightarrow {}^3T_{2g}$	Oh
	286	34,965	2278	Intra-ligand	
	345	28,986	1489	Intra-ligand	
[Cd(HL) <sub>2</sub> (N <sub>3</sub> ) <sub>2</sub> ].2H <sub>2</sub> O	354	28,249	962	Intra-ligand	Oh
	286	34,965	2276	Intra-ligand	
	345	28,986	1485	Intra-ligand	
[Hg(HL) <sub>2</sub> (N <sub>3</sub> ) <sub>2</sub> ].3H <sub>2</sub> O	354	28,249	960	Intra-ligand	Oh
	284	35,211	2274	Intra-ligand	
	345	28,986	2085	Intra-ligand	
	354	28,249	1266	Intra-ligand	

transitions and suggested geometries. The electronic spectra for all mixed ligand complexes displayed three absorption peaks in the ultraviolet region. The first peak at range (281 - 297) nm (35587 - 33670)  $\text{cm}^{-1}$  ( $\epsilon_{\text{max}} = 2370 - \epsilon_{\text{max}} = 2218$ )  $\text{mol}^{-1}\cdot\text{L}\cdot\text{cm}^{-1}$ , the second peak at (345, 347) nm (28986, 28818)  $\text{cm}^{-1}$  ( $\epsilon_{\text{max}} = 1152 - \epsilon_{\text{max}} = 2278$ )  $\text{mol}^{-1}\cdot\text{L}\cdot\text{cm}^{-1}$ , the third peak at (354 - 365) nm (28249 - 27397)  $\text{cm}^{-1}$  ( $\epsilon_{\text{max}} = 842 - \epsilon_{\text{max}} = 1324$ )  $\text{mol}^{-1}\cdot\text{L}\cdot\text{cm}^{-1}$  were attributed to intra-ligand  $\pi \rightarrow \pi^*$ ,  $n \rightarrow \pi^*$ , and  $n \rightarrow \pi^*$ , respectively [25] which exhibited bathochromic shift or hypsochromic shift when it comparison with that of free ligand (HL).

### 3.2.5. $[\text{Mn}(\text{HL})_2(\text{N}_3)_2(\text{H}_2\text{O})_2]\cdot\text{H}_2\text{O}$

The UV-Vis spectrum of Mn(II) complex, displayed three additional absorption peaks. The first peak at (475) nm (21053)  $\text{cm}^{-1}$  ( $\epsilon_{\text{max}} = 208$ )  $\text{mol}^{-1}\cdot\text{L}\cdot\text{cm}^{-1}$ , the second peak at (638) nm (15674)  $\text{cm}^{-1}$  ( $\epsilon_{\text{max}} = 41$ )  $\text{mol}^{-1}\cdot\text{L}\cdot\text{cm}^{-1}$ , the third peak at (794) nm (12594)  $\text{cm}^{-1}$  ( $\epsilon_{\text{max}} = 7$ )  $\text{mol}^{-1}\cdot\text{L}\cdot\text{cm}^{-1}$  were attributed to (d-d) spin-forbidden electronic transition type  ${}^6\text{A}_{1g} \rightarrow {}^4\text{T}_{2g(\text{G})}$ ,  ${}^6\text{A}_{1g} \rightarrow {}^4\text{T}_{1g(\text{G})}$ , and  ${}^6\text{A}_{1g} \rightarrow {}^4\text{E}_{g(\text{D})}$ , confirming octahedral geometry about Mn(II) [27].

### 3.2.6. $[\text{Co}(\text{HL})_2(\text{N}_3)_2]\cdot 2\text{H}_2\text{O}$

The electronic spectrum of Co(II) complex, showed two additional absorption peaks. The first peak at (650) nm (15,387)  $\text{cm}^{-1}$  ( $\epsilon_{\text{max}} = 13$ )  $\text{mol}^{-1}\cdot\text{L}\cdot\text{cm}^{-1}$ , and the second peak at (879) nm (11377)  $\text{cm}^{-1}$  ( $\epsilon_{\text{max}} = 4$ )  $\text{mol}^{-1}\cdot\text{L}\cdot\text{cm}^{-1}$  were attributed to (d-d) spin-allowed electronic transition type  ${}^4\text{T}_{1g} \rightarrow {}^4\text{A}_{2g}$ , and  ${}^4\text{T}_{1g} \rightarrow {}^4\text{T}_{2g}$ , respectively, characteristic octahedral geometry around Co(II) [28].

### 3.2.7. $[\text{Ni}(\text{HL})_2(\text{N}_3)_2]\cdot\text{H}_2\text{O}$

The UV-Vis spectrum of Ni(II) complex, displayed three additional absorption peaks. The first peak at (426) nm (23,474)  $\text{cm}^{-1}$  ( $\epsilon_{\text{max}} = 323$ )  $\text{mol}^{-1}\cdot\text{L}\cdot\text{cm}^{-1}$ , the second peak at (792) nm (15942)  $\text{cm}^{-1}$  ( $\epsilon_{\text{max}} = 10$ )  $\text{mol}^{-1}\cdot\text{L}\cdot\text{cm}^{-1}$ , the third peak at (879) nm (11,377)  $\text{cm}^{-1}$  ( $\epsilon_{\text{max}} = 2$ )  $\text{mol}^{-1}\cdot\text{L}\cdot\text{cm}^{-1}$  were due to (d-d) spin-allowed electronic transition type  ${}^3\text{A}_{1g} \rightarrow {}^3\text{T}_{1g(\text{P})}$ ,  ${}^3\text{A}_{1g} \rightarrow {}^3\text{T}_{1g}$ , and  ${}^3\text{A}_{1g} \rightarrow {}^3\text{T}_{2g}$ , respectively, which were a good agreement for octahedral geometry of Ni(II) complexes [29].

### 3.2.8. $[\text{Zn}(\text{HL})_2(\text{N}_3)_2]\cdot 3\text{H}_2\text{O}$ , $[\text{Cd}(\text{HL})_2(\text{N}_3)_2]\cdot 2\text{H}_2\text{O}$ , and $[\text{Hg}(\text{HL})_2(\text{N}_3)_2]\cdot 3\text{H}_2\text{O}$

The electronic spectra of Zn(II), Cd(II), and Hg(II), respectively show no absorption peaks in the visible region, indicating ( $d^{10}$ -system) for Zn(II), Cd(II), and Hg(II), that is mean no d-d electronic transition happened [27].

## 3.3. Biological Activity of the Ligand (HL) and Mixed Ligand Complexes

Indicating that the new ligand and its mixed ligand complexes exhibited antibacterial activity against four kinds of bacterial: *Staphylococcus aureus*, *Bacillus*, *Escherichia coli*, and *Pseudomonad aureus* respectively, in **Table 6**, **Figure 1** and **Figure 2**. The enhanced activity of the complexes can be explained on the bases of Overtone's concept and Tweedy's chelation theory [30] [31].

**Table 6.** Showed the inhibition circle diameter in millimeter for the bacteria after 24 hour in cubation paid (37°C) for ligand (HL) and its mono and mated complexes.

Compounds	<i>E. coli</i>	<i>Pesudomonas</i>	<i>Bacillus</i>	<i>Staphylococcus</i>
DMSO	5	7	-	5
Ligand (HL)	13	14	12	11
$[\text{Mn}(\text{HL})_2(\text{N}_3)_2(\text{H}_2\text{O})_2]\cdot\text{H}_2\text{O}$	-	11	-	15
$[\text{Co}(\text{HL})_2(\text{N}_3)_2]\cdot 2\text{H}_2\text{O}$	14	-	-	11
$[\text{Ni}(\text{HL})_2(\text{N}_3)_2]\cdot 3\text{H}_2\text{O}$	13	10	-	11
$[\text{Zn}(\text{HL})_2(\text{N}_3)_2]\cdot 3\text{H}_2\text{O}$	13	11	21	11
$[\text{Cd}(\text{HL})_2(\text{N}_3)_2]\cdot 2\text{H}_2\text{O}$	16	16	32	18
$[\text{Hg}(\text{HL})_2(\text{N}_3)_2]\cdot 3\text{H}_2\text{O}$	26	11	26	12

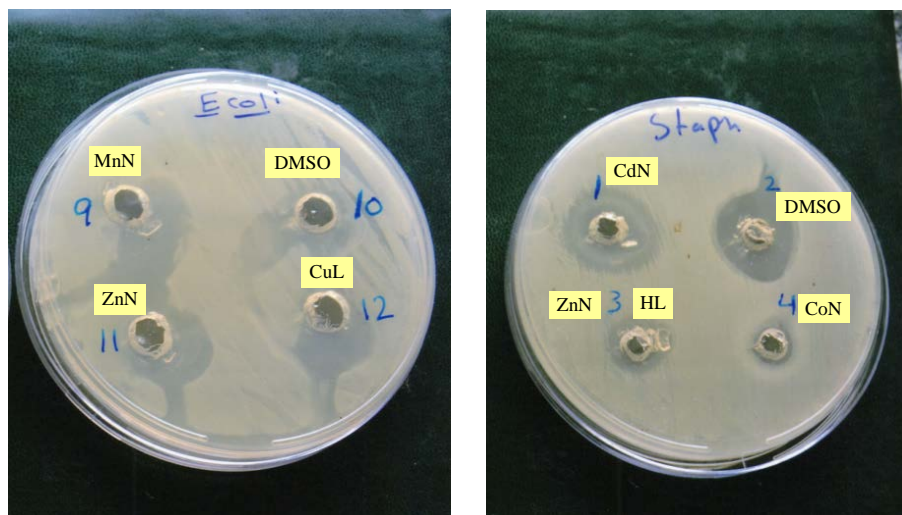


**Figure 1.** Inhibition diameter for ligands and complexes *E. coli* = *Escherichia coli*, Staph = *Staphylococcus aureus*.

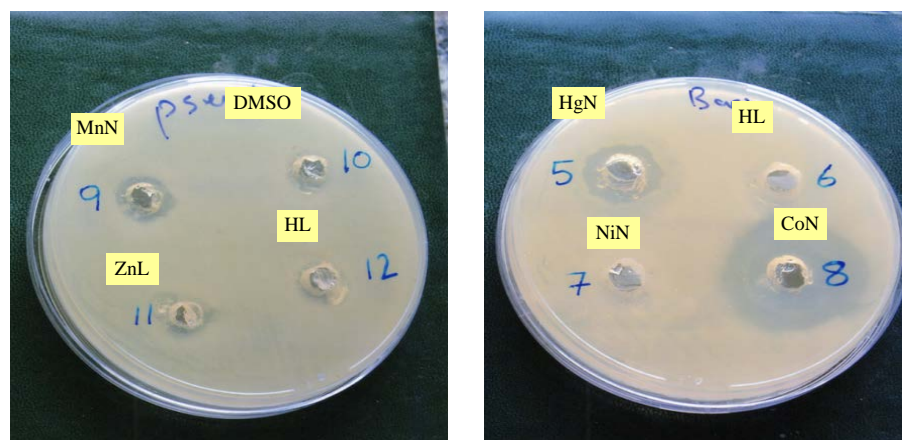


**Figure 2.** Inhibition diameter for ligands and complexes Pse = *Pseudomonas*, Bacil = *Bacillus*.

#### 4. Conclusions and the Proposed Molecular Structure for All Prepared Complexes

According to the characterization data for new Schiff base (HL) derived from 4-aminoantipyrine with glyoxylic acid, and its mixed ligand complexes based Schiff base ligand HL primary ligand and azide ion ( $N_3^-$ ) (co-ligand), by FT-IR, UV-Vis, atomic absorption,  $^1H$  NMR,  $^{13}C$  NMR, magnetic susceptibility, molar conductivity, elemental microanalysis, chloride content along with melting point, we found that:

1) The Schiff base (HL) in mixed ligand complexes behaved bidentate ligand through its azomethine nitrogen, oxygen atom of C=O group of five member ring with the central metal ions: Co(II), Ni(II), Zn(II), Cd(II) and Hg(II) forming complexes with molecular formula:  $[M(HL)_2(N_3)_2] \cdot mH_2O$  where: ( $M^{II} = Co, Cd; m = 2$ ), ( $M^{II} = Ni, Zn, Hg; m = 3$ ), except in Mn(II) complex, Schiff base (HL) behaved monodentate ligand via azomethine nitrogen forming complex with molecular formula  $[Mn(HL)_2(N_3)_2] \cdot H_2O$ .

2) The octahedral geometrical structure was suggested for all prepared complexes based on the characterization data for all technique.

3) The antibacterial study showed that the complexes were more toxic to the strain of bacteria taken under study than the Schiff base ligand (HL).

#### References

- [1] Mehta, B.H. and Chavan, V.L. (2011) X-Ray, Thermal and Biological Studies of Ru(III), Rh(III) and Pd(II) Schiff



- Base Metal Complexes. *Research Journal of Chemistry and Environment*, **15**, 57-61.
- [2] Raman, N., Raja, S.J. and Salkthivel, A. (2009) Transition Metal Complexes with Schiff-Base Ligands: 4-Aminoantipyrine Based Derivatives—A Review. *Journal of Coordination Chemistry*, **62**, 691-709. <http://dx.doi.org/10.1080/00958970802326179>
- [3] Rosu, T. Pahontu, E., Maxim, C., Georgescu, R., Stanica, N. and Gulea, A. (2011) Some New Cu(II) Complexes Containing an on Donor Schiff Base: Synthesis, Characterization and Antibacterial Activity. *Polyhedron*, **30**, 154-162. <http://dx.doi.org/10.1016/j.poly.2010.10.001>
- [4] Mohamed, G.G., Omar, M.M. and Ibrahim, A.A. (2009) Biological Activity Studies on Metal Complexes of Novel Tridentate Schiff Base Ligand. Spectroscopic and Thermal Characterization. *European Journal of Medicinal Chemistry*, **44**, 4801-4812. <http://dx.doi.org/10.1016/j.ejmech.2009.07.028>
- [5] Elemike, E.E. Oviawe A.P. and Otuokere, I.E. (2011) Potentiation of the Antimicrobial Activity of 4-Benzylimino-2,3-Dimethyl-1-phenylpyrazal-5-one by Metal Chelation. *Research Journal of Chemical Sciences*, **1**, 6-11.
- [6] Agarwal, R.K., Singh, I. and Sharma, D.K. (2006) Synthesis, Spectral, and Biological Properties of Copper(II) Complexes of Thiosemicarbazones of Schiff Bases Derived from 4-Aminoantipyrine and Aromatic Aldehydes. *Bioinorganic Chemistry and Applications*, **2006**, 1-10.
- [7] Acheson, R.M. (2009) Introduction to Heterocyclic Compounds. 4th Edition, Wiley, New York.
- [8] Gopalakrishnan, S. and Joseph, J. (2009) Antifungal Activities of Copper (II) with Biosensitive Macrocyclic Schiff Base Ligands Derived from 4-Aminoantipyrine Derivatives. *Microbiology*, **37**, 141-146.
- [9] Mishchenko, A.V. Lukov V.V. and Popov, L.D. (2011) Synthesis and Physico-Chemical Study of Complexation of Glyoxylic Acid Aroylhydrazones with Cu(II) in Solution and Solid Phase. *Journal of Coordination Chemistry*, **64**, 1963-1976. <http://dx.doi.org/10.1080/00958972.2011.585640>
- [10] Kramer, D.N., Klein, N. and Baselice, R.A. (1999) Quantitative Determination of Glyoxylic Acid. *Analytical Chemistry*, **31**, 250-252. <http://dx.doi.org/10.1021/ac60146a028>
- [11] Sokol, H.A. (1977) Determination of Pyruvic and Glyoxylic Acids in the Presence of Acetaldehyde. *Analytica Chimica Acta*, **89**, 407-408. [http://dx.doi.org/10.1016/S0003-2670\(01\)84741-3](http://dx.doi.org/10.1016/S0003-2670(01)84741-3)
- [12] Tharmaraj, P., Kodimunthiri, D., Sheela, C.D. and Shanmugapriya, C.S. (2009) Synthesis, Spectral Studies and Antibacterial Activity of Cu(II), Co(II) and Ni(II) Complexes of 1-(2-Hydroxyphenyl)-3-phenyl-2-propen-1-one) $N^2$ -[(3,5-dimethyl-1H-pyrazol-1-yl)methyl] Hydrazone. *Journal of the Serbian Chemical Society*, **74**, 927-938. <http://dx.doi.org/10.2298/JSC0909927T>
- [13] Suresh, M.S. and Prakash, V. (2010) Preparation and Characterization of Cr(III), Mn(II), Co(II), Ni(II), Cu(II), Zn(II) and Cd(II) Chelates of Schiff's Base Derived from 4-Aminoantipyrine. *International Journal of Physical Sciences*, **5**, 2203-2211.
- [14] Anupama, B., Padmaja, M. and Kumari, C.G. (2012) Synthesis, Characterization, Biological Activity and DNA Binding Studies of Metal Complexes with 4-Aminoantipyrine Schiff Base Ligand. *E-Journal of Chemistry*, **9**, 389-400. <http://dx.doi.org/10.1155/2012/291850>
- [15] Raman, N., Sobha, S. and Selvaganapathy, M. (2012) Probing the DNA Binding Mode of Transition Metal Based Biologically Active Compounds: Validation by Spectroscopic Methods. *International Journal of Pharma and Bio Sciences*, **3**, 251-268.
- [16] Manjula, B. and Antony, S.A. (2013) Arsenic Induced Biochemical Changes in *Perna viridis* as Potential Biomarkers in Metal Pollution. *Asian Journal of Biochemical and Pharmaceutical Research*, **3**, 168-178.
- [17] Wang, X.Y., Wang, Z.M. and Gao, S. (2008) Constructing Magnetic Molecular Solids by Employing Three-Atom Ligands as Bridges. *Chemical Communications*, **2008**, 281-294. <http://dx.doi.org/10.1039/B708122G>
- [18] Ju, Z.F., Yao, Q.X., Wu, W. and Zhang, I. (2008) Strong Electron-Accepting Methyl Viologen Dication Confined in Magnetic Hosts: Synthesis, Structural, Characterization, Charge-Transfer and Magnetic Properties, of [(MV) $_2$ [Ni(SCN) $_3$ ].Cl.2H $_2$ O] $_n$  and [(MV)[M(N $_3$ ) $_2$ (SCN) $_2$ ]] (M=Mn, Co). *Dalton Transactions*, 355-362. <http://dx.doi.org/10.1039/B710628A>
- [19] Belaid, S., Landreau, A., Djebbar, S., Benali-Baitich, O., Bouet, G. and Bouchara, J. (2008) Synthesis, Characterization and Antifungal Activity of a Series of Manganese(II) and Copper(II) Complexes with Ligands Derived from Reduced N,N-O-phenylene bis(salicylideneimine). *Journal of Inorganic Biochemistry*, **102**, 63-69. <http://dx.doi.org/10.1016/j.jinorgbio.2007.07.001>
- [20] El-Asmy, A.A., Al-Ansi, T.Y. and Shaiba, Y.M. (1989) Chelated Complexes of Cadmium(II), Cobalt(II), Copper(II), Mercury(II), Nickel(II), Uranyl(II) and Zinc(II) with Benzil bis(4-phenylthiosemicarbazone). *Transition Metal Chemistry*, **14**, 446-452. <http://dx.doi.org/10.1007/BF01092587>
- [21] Socrates, G. (1980) Infrared Characteristic Group Frequencies. Wiley, New York.

- [22] Raj, K.D. and Sharad, K.M. (2011) Synthesis, Spectroscopic (IR, Electronic, Fab-Mass, and PXRD), Magnetic and Antimicrobial Studies of New Iron(III) Complexes Containing Schiff Bases and Substituted Benzoxazole Ligands. *Journal of Coordination Chemistry*, **64**, 2292-2301. <http://dx.doi.org/10.1080/00958972.2011.594886>
- [23] Nakamoto, K. (1978) *Infrared and Raman Spectra of Inorganic and Coordination Compounds*. 3rd Edition, Wiley, New York.
- [24] Cowley, A.R. Dilworth, J.R. Donnelly, P.S. and Whilte, J.M. (2006) Copper Complexes of Thiosemicarbazone-Pyridylhydrazine (THYNIC) Hybrid Ligands: A New Versatile Potential Bifunctional Chelator for Copper Radiopharmaceuticals. *Inorganic Chemistry*, **45**, 496-498. <http://dx.doi.org/10.1021/ic0514492>
- [25] Al-Hamdani, A.A.S. and Shaker, S.A. (2011) Synthesis, Characterization, Structural Studies and Biological Activity of a New Schiff Base-Azo Ligand and Its Complexation with Selected Metal Ions. *Oriental Journal of Chemistry*, **27**, 835-845.
- [26] Lever, A.B.P. (1984) *Inorganic Electronic Spectroscopy*. 2nd Edition, Elsevier, New York.
- [27] Huheey, J.E. (1994) *Inorganic Chemistry: Principles of Structure and Reactivity*. Harper and Row Publisher, New York.
- [28] Awetz, J., Melnick, P. and Delbrgs, A. (2007) *Medical Microbiology*. 4th Edition, McGraw Hill, New York.
- [29] Priya, N.P., Arunachalam, S.V., Sathya, N., Chinnusamy, V. and Jayabalakrishnan, C. (2009) Catalytic and Antimicrobial Studies of Binuclear Ruthenium(III) Complexes, Containing Bis- $\beta$ -Diketones. *Transition Metal Chemistry*, **34**, 437-445. <http://dx.doi.org/10.1007/s11243-009-9214-z>
- [30] Jayablakrishnan, C. and Natarajan, K. (2002) Synthesis, Characterization, and Biological Activities of Ruthenium(II) Carbonyl Complexes Containing Bifunctional Tridentate Schiff Bases. *Transition Metal Chemistry*, **27**, 75-79. <http://dx.doi.org/10.1023/A:1013437203247>
- [31] Tweedy, B.G. (1964) Plant Extracts with Metal Ions as Potential Antimicrobial Agents. *Phytopatology*, **55**, 910-918.